

Fabry–Perot refractometer based on an end-of-fiber polymer tip

O. Frazão,^{1,2,*} P. Caldas,^{1,2} J. L. Santos,^{1,2} P. V. S. Marques,^{1,2} C. Turck,³ D. J. Lougnot,³ and O. Soppera^{3,4}

¹INESC Porto, Rua do Campo Alegre, 687, 4169-007 Porto, Portugal

²Departamento de Física, Faculdade de Ciências da Universidade do Porto, Rua do Campo Alegre, 687, 4169-007 Porto, Portugal

³Departamento de Photochimie Générale, CNRS FRE 3252, ENSCMu, 34 Rue Marc Seguin, 68093 Mulhouse Cedex, France

⁴olivier.soppera@uha.fr

*Corresponding author: ofraza@inescporto.pt

Received May 26, 2009; revised June 19, 2009; accepted July 6, 2009;
posted July 15, 2009 (Doc. ID 111757); published August 11, 2009

A micrometric Fabry–Perot refractometer based on an end-of-fiber polymer tip is proposed. The fiber tip, with a length of 36 μm , was fabricated by self-guiding photopolymerization. The two-wave interferometric operation was achieved by combining the light waves generated at the interface between the single-mode fiber and the polymer tip, and at the fiber tip end (Fresnel reflection). The Fabry–Perot interferometer is coherence addressed and heterodyne interrogated, resulting into a liquid refractive index resolution of $\approx 7.5 \times 10^{-4}$. © 2009 Optical Society of America
OCIS codes: 060.0060, 060.2370, 120.2230.

The measurement of chemical and biochemical parameters in a wide variety of environments is recognized to be an increasingly important challenge for sensing technologies in general, and for those based on optical devices in particular [1]. The use of optical fibers as intrinsic sensing platforms is highly attractive owing to their small size and possibility of remote and multiplexed operation [2].

Optical sensing of chemical and biochemical parameters relies on two fundamental concepts, namely, fluorescence and evanescent field interaction [3]. The latter one is based on the partial evanescent overlap of a guided electromagnetic wave with a medium. In this case, the refractive index, whose changes reflect the variations in the parameter under measurement, is read using interferometry. The efficiency of this approach depends on the penetration depth of the evanescent field in the medium. Owing to this, sensing heads with large intrinsic penetration were developed. Some specific configurations rely on *D*-type fibers, which favor the contact between the fiber core and the medium, have been reported previously [4].

Fiber Fabry–Perot interferometers (FFPIs) have been extensively explored for sensing applications [2]. In particular, the literature dealing with the application of this structure as temperature, pressure, and flow sensors is abundant [5–7]. One of the most crucial issues is the fabrication of the two in-fiber reflectors. Various methods and technologies were reported, such as dielectric thin-films [8], fiber Bragg gratings [9], or UV-induced mirrors [10]. The technique used in this work to implement a polymer Fabry–Perot cavity relies on self-guided photopolymerization, a process introduced to fabricate microtips at the end of optical fibers [11,12]. The photopolymerizable material was chosen to provide low edge rugosity and suitable optical and mechanical properties. The photonic parameters were adapted to

obtain a flat end that is important to ensure an optimum optical response.

When the FFPI is implemented at the fiber end, quite simply, one of the interfering beams can be created by the Fresnel reflection at this end. Also, if in the interferometer length, the fiber diameter is reduced relatively to the standard value, a reflected wave is created at the polymer/fiber interface owing to the mismatch of the effective refractive index of the guided mode between these two regions. The end-of-fiber diameter reduction can be effectively achieved utilizing photopolymerization techniques [12]. Also, if this diameter reduction is such that the fiber core is exposed to the external medium, then the guided mode will have a large evanescent field in this medium, rendering the FFPI sensitive to its refractive index. The aim of this Letter is to exemplify the potential of this concept.

The fabrication process of the tip consisted in the deposition of a liquid photopolymerizable formulation at the end of an optical fiber. The droplet was then exposed to 532 nm laser light to induce polymerization (the laser light is guided by the fiber) [13]. The physico-chemical and photonic parameters were optimized so as to achieve a flat end–tip surface, which is important for generating one of the two interfering FFPI waves (on account of the weak reflectivity of this end surface, multiple reflections can be disregarded). After exposure and rinsing off the unreacted formulation with ethanol, a polymer tip appeared at the end of the fiber. This tip (Fig. 1) is $\approx 36 \mu\text{m}$ cavity length with a diameter of $\approx 7 \mu\text{m}$.

To detect the phase changes of the low-finesse fiber Fabry–Perot interferometer, a second interferometer was built to implement coherence addressing [14]. As shown in Fig. 1, this is a conventional fiber Michelson interferometer with an open-air path in one of its arms, which is adjusted to match the optical path difference of the FFPI (the optical path unbalance,

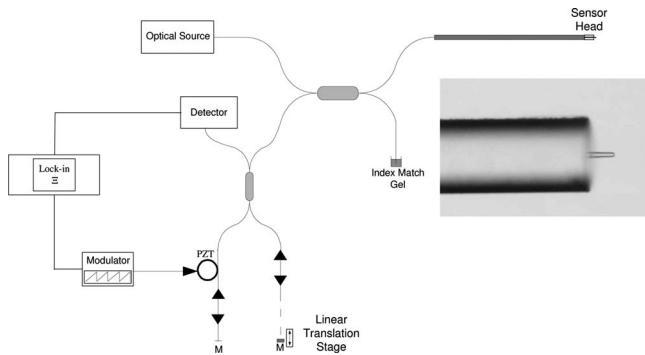


Fig. 1. Experimental setup and photo of the sensing head.

$\approx 105 \mu\text{m}$, is larger than the coherence length of the optical source). The fiber in the other arm of the receiving interferometer was wound around a ring-shaped piezoelectric transducer (PZT) that is modulated with an electrical sawtooth waveform with the amplitude adjusted to obtain a signal at the photodetection suitable for pseudoheterodyne processing. The light source used was a superluminescent diode operating at 1320 nm with a spectral width of $\approx 35 \text{ nm}$ (i.e., a coherence length of $L_c \approx 33 \mu\text{m}$). After adequate electronic filtering, this signal had the form of an electric carrier with a phase that mirrors the optical phase of the tandem interferometric system. This heterodyne technique is known to provide sensitive interferometric phase reading [15].

Figure 2 presents the spectral transfer function of the FFPI modulated by the spectral distribution of the optical power source. When this modulation is corrected, a normalized interferometric spectral response is obtained (shown in the figure inset).

To calibrate the sensing head for liquid refractive index measurements, the interferometric tip sensor was immersed in samples of water containing various percentages of ethylene glycol. These samples were characterized with an Abbe refractometer using the sodium D line (589 nm). Because the sensing head was operating at 1300 nm , it was necessary to use the Cauchy equation with the appropriated coefficients to correct the refractive index at this wavelength [16].

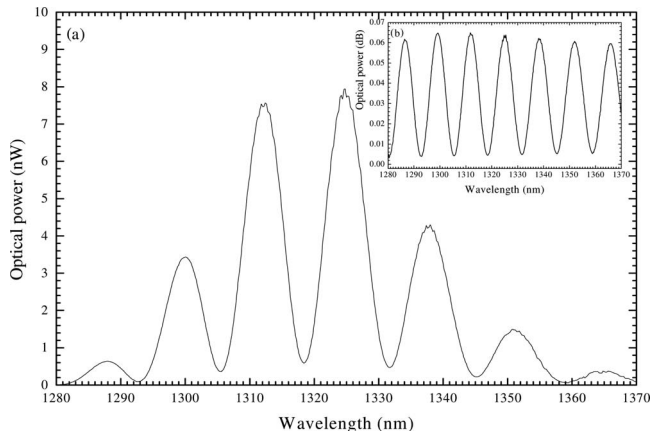


Fig. 2. (a) Spectral response of the tip FFPI sensor tailored by the source spectral distribution, (b) normalized spectral response (the periodicity of the channeled spectrum is 13 nm).

The modification of the refractive index of the liquid sample induces a change in the effective refractive index of the guided mode in the fiber tip, a result of a substantial fraction of the optical field that propagates in the liquid. Therefore, the interferometric phase also changes, as shown in Fig. 3. As can be observed, the dependence is approximately linear, with a coefficient of $4.65/0.001^\circ/(\text{RI})$ refractive index change. To check the ultimate achievable resolution, increasing percentages of ethylene glycol were added to water so that the refractive index of the mixture proceeds stepwise from 1.333 (pure water) to 1.450 with index increments of 1.5×10^{-2} . The corresponding phase behavior is reported in Fig. 4, which shows a step phase variation in $\sim 70^\circ$. The phase fluctuations in the regions of constant liquid refractive index are due to the slight temperature fluctuations, particularly when the liquids are mixed to induce the step change (fluctuation of $\sim 19^\circ$). Considering the sensitivity value and the average peak-to-peak phase fluctuation in the region before the step change ($\approx 7^\circ$), the refractive index resolution limit turns out to be $\pm 7.5 \times 10^{-4}$.

The ultimate sensitivity of this device is subjected to substantially reducing the phase fluctuations related to temperature unstabilities. Thus, damping the peak-to-peak fluctuations of the interferometric phase down to 0.1° would push the refractive index resolution down to $\pm 1.1 \times 10^{-5}$.

This performance makes this sensing system appealing for many applications involving refractive index measurements in liquids, particularly if the reduced dimensions of the sensor head, both in diameter (less than $10 \mu\text{m}$) and length (some tens of micrometers) are taken into consideration.

A fiber Fabry–Perot interferometer based on an end-of-fiber polymer tip was described, and the potential of this structure for refractive index measurement of the surrounding medium was demonstrated. Using this simple implementation procedure, a refractive index resolution of $\text{ca } \sim 7.5 \times 10^{-4}$ could be achieved, but substantially better values should be possible. In view of its performance and micrometric size, it is foreseen that the proposed sensing head

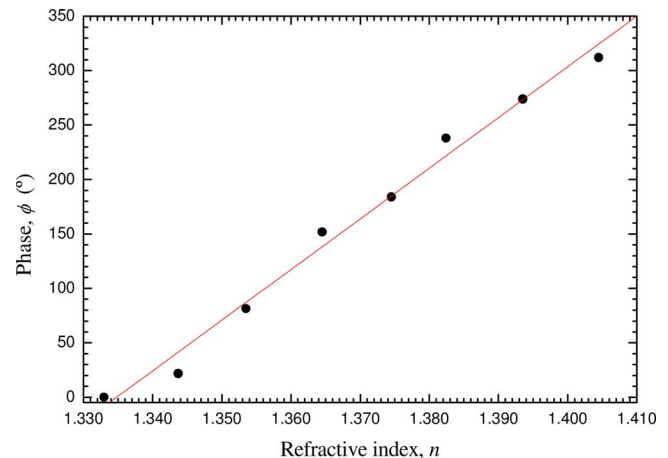


Fig. 3. (Color online) Relationship between the FFPI interferometric phase and the refractive index of the surrounding liquid.

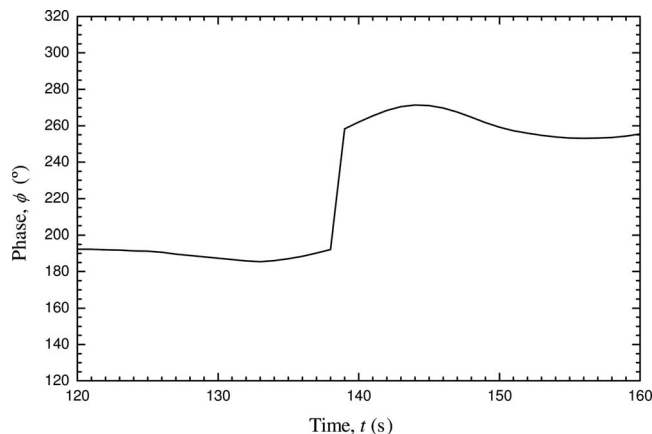


Fig. 4. FFPI phase step change induced by a surrounding liquid refractive index step change in $\delta n = 1.5 \times 10^{-2}$.

will be attractive for applications in the chemical and biochemical domains, including environmental monitoring. Moreover, its great simplicity of use associated to a derisory cost of fabrication and implementation might well result in the design of disposable sensors.

References

1. O. S. Wolfbeis, *Anal. Chem.* **76**, 3269 (2004).
2. J. M. Lopez-Higuera, *Handbook of Optical Fibre Sensing Technology* (Wiley, 2002).
3. C. R. Taitt, G. P. Anderson, and F. S. Ligler, *Biosens. Bioelectron.* **20**, 2470 (2005).
4. M.-H. Chiu, S.-N. Hsu, and H. Yang, *Sens. Actuators B* **101**, 322 (2004).
5. Y. Z. Zhu and A. B. Wang, *IEEE Photon. Technol. Lett.* **17**, 447 (2005).
6. B. Qi, G. R. Pickrell, P. Zhang, Y. Duan, W. Peng, J. Xu, Z. Huang, J. Deng, H. Xiao, Z. Wang, W. Huo, G. R. May, and A. Wang, *Proc. SPIE* **4578**, 182 (2002).
7. W. Peng, G. R. Pickrell, Z. Huang, J. Xu, D. W. Kim, B. Qi, and A. Wang, *Appl. Opt.* **43**, 1752 (2004).
8. C. E. Lee and H. F. Taylor, *Electron. Lett.* **24**, 193 (1988).
9. P. Betts and J. A. Davis, *Opt. Eng.* **43**, 1258 (2004).
10. F. Shen, W. Peng, K. L. Cooper, G. Pickrell, and A. Wang, *Proc. SPIE* **5590**, 47 (2004).
11. R. Bachelot, P. Royer, G. Wurtz, C. Ecoffet, A. Espanet, and D. J. Lougnot, French Patent No. PCT 9814385, 2001.
12. O. Soppera, S. Jradi, and D. J. Lougnot, *J. Polym. Sci. Part A Polym. Chem.* **46**, 3783 (2008).
13. S. Jradi, O. Soppera, and D. J. Lougnot, *Appl. Opt.* **47**, 3987 (2008).
14. J. L. Brooks, R. H. Wentworth, R. C. Youngquist, M. Tur, B. Y. Kim, and H. J. Shaw, *J. Lightwave Technol.* **3**, 1062 (1985).
15. D. A. Jackson, A. D. Kersey, and J. D. C. Jones, *Electron. Lett.* **18**, 1081 (1982).
16. D. A. Pereira, O. Frazão, and J. L. Santos, *Opt. Eng.* **43**, 299 (2004).